

# Effect of particle size and volume fraction of the reinforcement on the microstructure and mechanical properties of friction welded MMC to AA 6061 aluminum alloy

I. Kirik<sup>1\*</sup>, N. Ozdemir<sup>2</sup>, U. Caligulu<sup>2</sup>

<sup>1</sup>*Batman University, Faculty of Engineering and Architecture, Department of Metallurgical and Materials Engineering, 72060 Batman, Turkey*

<sup>2</sup>*Fırat University, Faculty of Technology, Department of Metallurgical and Materials Engineering, Elazığ, Turkey*

Received 4 March 2012, received in revised form 3 October 2012, accepted 5 October 2012

## Abstract

The aim of this study is to evaluate the welding characteristic of friction welded dissimilar joints of an aluminum matrix composite Al-5%Cu-SiCp to AA 6061 aluminum alloy. Specimens of 12 mm diameter were used to fabricate the joints. The friction welding tests were carried out using a direct-drive type friction welding machine. After friction welding, the joining performance of the aluminum matrix composite Al-5%Cu-SiCp to AA 6061 friction welded joints was studied, and the effect of the particle size on the microstructure and mechanical properties of the friction welded joints was also estimated. The experimental results indicate that aluminum matrix composite and AA 6061 aluminum alloy can be joined, eventually, the particle size and volume fraction of the reinforcement play the major role in the tensile strength of friction welded joints.

**Key words:** friction welding, metal matrix composites, mechanical properties

## 1. Introduction

SiCp reinforced aluminum metal matrix composites (SiCp/Al MMCs) have a unique combination of mechanical and physical properties, such as high specific strength and specific modulus of elasticity, low thermal expansion coefficient and good wear resistance [1]. The main limitation of these materials is their low weldability by conventional fusion welding techniques (such as TIG, MIG, laser and electron beam), since they produce major microstructural modifications in the welds (interfacial matrix-particle reactions, particle segregation, etc.) which, in turn, significantly affect their mechanical properties [2]. Despite considerable improvements in developing Al-based composites, the lack of reliable joining methods currently restricts their wider application. Friction welding can be used to join metals of widely differing thermal and mechanical properties [3, 4].

Friction welding is a solid state joining process which can be used to join a number of different metals.

The process involves making welds, in which one component is moved relative to, and in pressure contact, with the mating component to produce heat at the faying surfaces. Softened material begins to extrude in response to the applied pressure, creating an annular upset. Heat is conducted away from the interfacial area for forging to take place. The weld is completed by the application of a forge force during or after the cessation of relative motion. The joint undergoes hot working to form a homogeneous, full surface, high-integrity weld. Friction welding is the only viable method in this field to overcome the difficulties encountered in the joining of dissimilar materials with a wide variety of physical characteristics. The advantages of this process are, among others, no melting, high reproducibility, short production time and low energy input [5–7]. Various recent studies have also reported on the weldability of metal matrix composites (MMCs), consisting of different base materials such as aluminum, copper and titanium and various reinforcements, Al<sub>2</sub>O<sub>3</sub>, SiC, TiC, Si<sub>3</sub>N<sub>4</sub> or B<sub>4</sub>C [8–11].

\*Corresponding author: [alihankirik@gmail.com](mailto:alihankirik@gmail.com)

Table 1. Chemical composition of the test materials

Material	Alloying elements (wt.%)								
	Al	Si	Mg	Fe	Cu	Cr	Mn	Ti	Bal
AA 6061	96.0	2.1	0.95	0.33	0.17	0.066	0.04	0.022	< 0.05

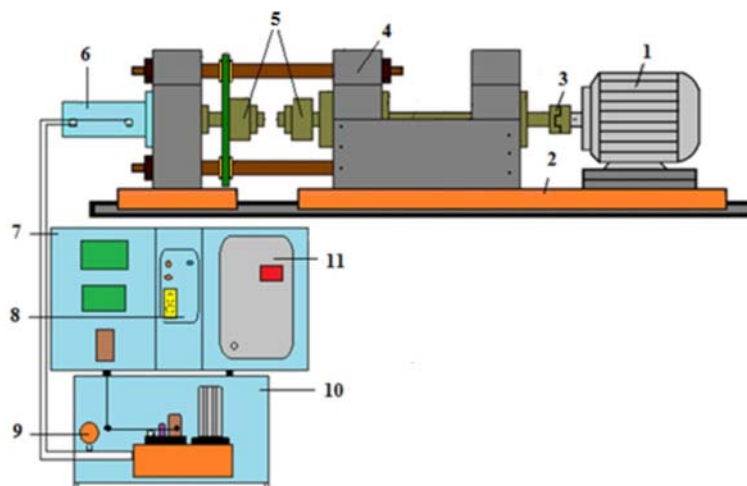


Fig. 1. Experimental set-up: 1 – electric motor, 2 – console, 3 – clutch, 4 – the moveable jaw hardware, 5 – jaws, 6 – hydraulic cylinder, 7 – electronic circuit equipment, 8 – control unit, 9 – manometer, 10 – hydraulic unit, 11 – inverter.

Table 2. Composition of MMC samples

Sample	Composition (wt.%)		
	SiCp/particle size	Cu	Al
S1	5/30 $\mu\text{m}$	5	90
S2	10/30 $\mu\text{m}$	5	85
S3	15/30 $\mu\text{m}$	5	80
S4	5/60 $\mu\text{m}$	5	90
S5	10/60 $\mu\text{m}$	5	85
S6	15/60 $\mu\text{m}$	5	80

The reinforcement particles clearly affect the welding process in different ways; reducing plasticity with respect to the unreinforced alloys, leading to a narrower range of the welding parameters [4].

In the literature, limited research has been made on the FW of Al-SiC particulate metal matrix composite. Thus, the objective of the present work is to examine the effect of particle size and volume fraction on the microstructure and mechanical properties of friction welded joints of conventionally hot pressed Al-5%Cu-SiC composite to AA 6061 aluminum alloy.

## 2. Experimental procedures

The composites used in the experiments were pro-



Fig. 2. Overview of friction welded SiCp reinforced aluminum composite to AA 6061 alloy.

duced by powder metallurgy. AA 6061 alloy powders were mixed with 30 and 60  $\mu\text{m}$  particulate SiCp in the volume fractions of 5, 10 and 15 % for both sizes separately. The mixtures were cold-pressed in a steel die under a pressure of 10 MPa and then hot-pressed under 5 MPa at 500  $^{\circ}\text{C}$  after degassing in a furnace. Finally, they were sintered at 550  $^{\circ}\text{C}$  for 60 min. The chemical composition of the matrix material and AA 6061 aluminum alloy is given in Table 1. Sintered parts were machined in a lathe to a diameter of 12 mm and a length of 50 mm for the friction welding. The counter-

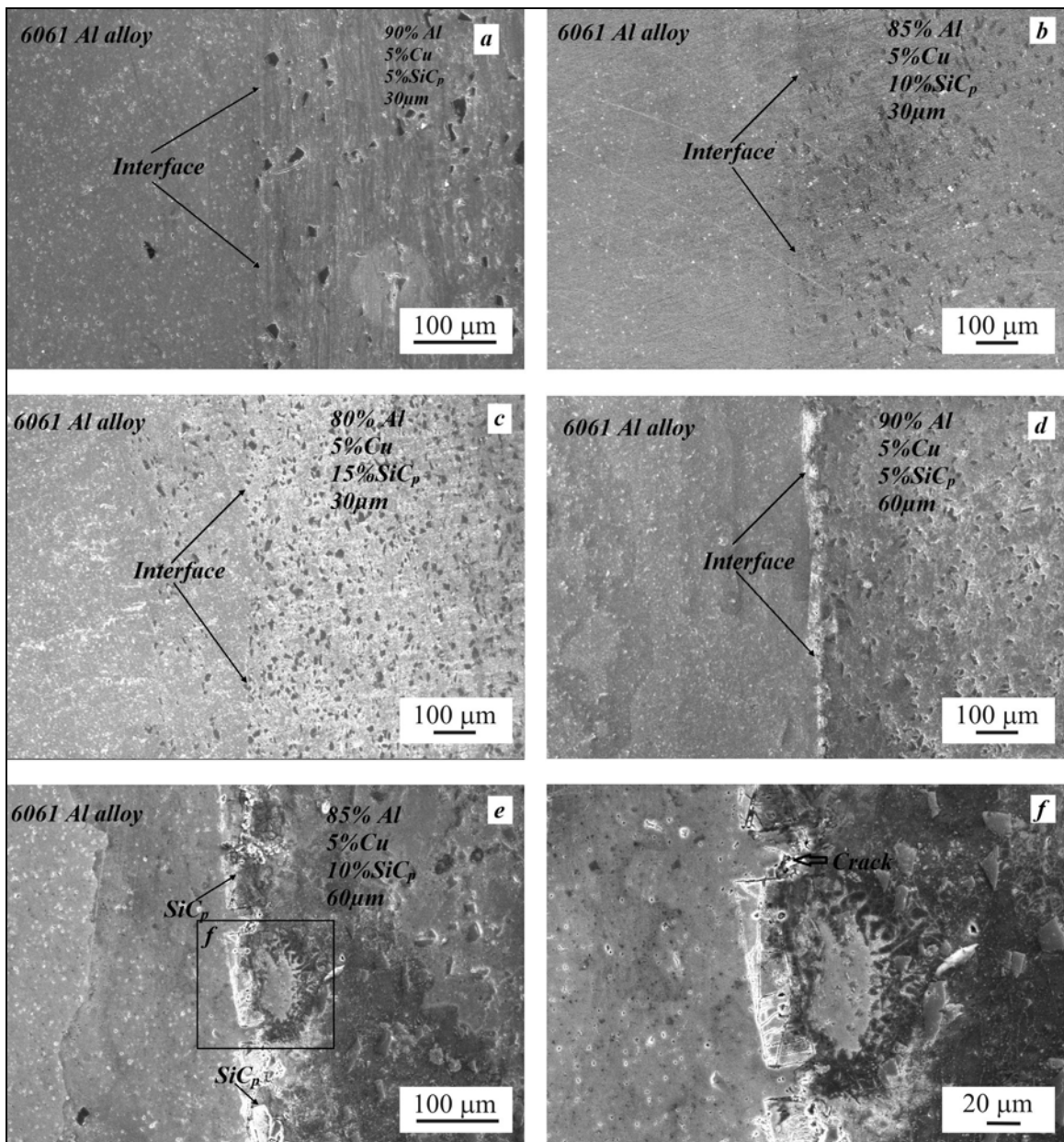


Fig. 3. SEM micrograph taken from the welding interface of the specimens S1 (a), S2 (b), S3 (c), S4 (d) and S5 (e, f), respectively.

part or AA 6061 aluminum alloy was delivered in bars with a diameter of 12 mm and machined in the same dimensions. Figure 1 illustrates experimental set-up.

In the present work, rotation speed of 1700 rpm, friction pressure of 15 MPa, forging pressure of 30 MPa and friction time of 8 s were used to produce the weld joints. Friction welding tests were carried out by direct-drive friction welding machine. After friction welding, in order to determine the microstructural changes that occurred, the interface regions of the welded specimens were examined by scanning electron microscopy (SEM), and energy dispersive spectrometry (EDS). Microhardness and tensile tests were conducted to determine mechanical properties of the

welded specimens. Tensile tests were conducted on an Instron test machine at room temperature with  $10^{-2}$  mm s<sup>-1</sup> cross-head rate. Microhardness measurements were carried out by a Leica microhardness tester under a load of 50 gf.

### 3. Results and discussion

#### 3.1. Evaluation of microstructures

The macro-view of specimens welded under different welding conditions is shown in Fig. 2. Visual examination of the welded specimens showed uniform weld

joints. The flash obtained was symmetric, which indicated plastic deformation on both the rotating and upsetting (reciprocating) sides. The integrity of the joints was evaluated for the friction-welded joints. The friction processed joints were sectioned perpendicular to the bond line and observed through the SEM microscope. It can be clearly seen that there were no cracks and voids in the weld interface. From the microstructural observations, the microstructures formed interface zone during or after FW processes, there are three distinct zones across the specimens identified as unaffected zone (UZ), deformed zone (DZ) and transformed and recrystallized fully plastic deformed zone (FPDZ). Typical grain refinement occurred in the DZ region by the combined effect of thermal and mechanical stresses. A typical micrograph showing the different morphologies of the microstructure at different zones of the friction processed joint is shown in Fig. 3.

The boundary and shape of these regions varied as a result of the relation between volume fraction and particle size. From the micrograph of heat affected zone (HAZ) taken from the interface zone of friction welded specimens, the formation of structure usually showed fine equiaxed grains and ductility in the weld zone (WZ). The WZ had a fine equiaxed grain structure. This structure was produced by dynamic recrystallization, which was caused by frictional heat and severe plastic deformation. An important consequence of friction welding on a composite material is that the reinforcing particles close to the bonding line can change their distribution compared with the base material region. This phenomenon explains why fractures occur early in the friction joining operation since the particles are retained at the bond line as a direct result of plasticized material flow. Fracture occurs as a direct result of the severe plastic deformation at relatively low temperatures imposed in the beginning of the friction joining process.

### 3.2. Tensile test results

The tensile test results are given in Fig. 4. As the volume fraction and the size of the SiCp particles increase, the tensile strength decreases. This can be explained by the increasing density of voids with increasing SiCp volume fraction. When the stress built up around particles reaches a critical value, ductility reduction, particle fracture or interface decohesion takes place. As a consequence, the matrix can support the load no longer. Friction welded joints presented the same fracture behavior, since the failures in joints were located in the composite side as seen in Fig. 5. Additionally, longer heating times and a slow cooling rate decreased the strength in friction welding. The joint strength decreased with an increasing volume fraction and particle size for all the specimens tested. When the composite material is subjected to load, the pres-

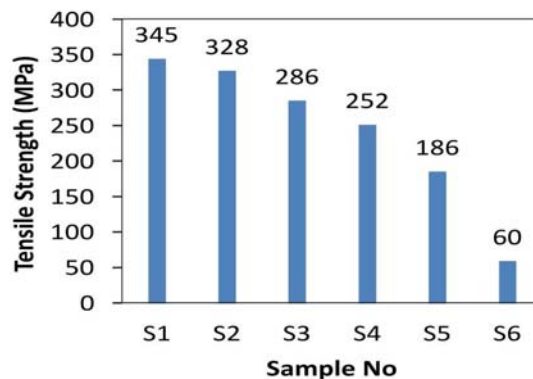


Fig. 4. Tensile strength of friction welded joints.



Fig. 5. Macro photograph – tensile test specimen.

ence of clusters and defects reduces ductility as these areas would fail prematurely. The above factors are attributed to the failure of material in the interface, i.e., HAZ.

### 3.3. Microhardness results

The microhardness values measured perpendicular to the weld interface on both sides of specimens S1-S6 are given in Fig. 5. The hardness in the central portion of the weld region was in the range 120–250 HV. The hardness in the deformed zone of the joints increased due to the increasing particle size and volume fraction. Moreover, the hardness values in the interface of the same volume ratio of the SiCp composites also increase with increasing particle size and volume fraction. Due to deformation during the welding process, in reinforcement phase, which has small SiCp particles sized S1, S2 and S3, specimens are more prone to overflow from the interface than those of larger particle phase. For large particle sized composites, following the deformation of the matrix during the friction, the ceramic, contacting the facing material, started to crack and embedded into the matrix again, under the axial pressure, without having a chance to even partially overflow. Eventually, it cracked and embedded into the matrix interface, these SiCp particles remain in the joint interfaces, thus causing a higher in-

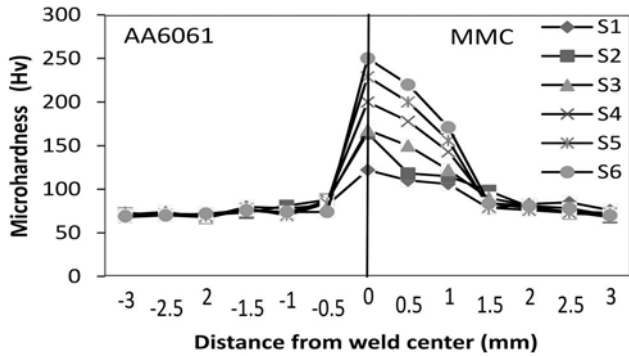


Fig. 6. Microhardness distribution across the welding interface of friction welded specimens.

crease in the microhardness as confirmed by the microhardness distribution values shown in the Fig. 6. Additionally, evaluating the macro images of these welded joints, a decrease is seen in the amount of the material overflowing from the MMCs side, depending on the increase in the particle size. From the microstructure images taken from the welding interface, after joining different MMCs which are prepared by reinforcing different SiCp particle size and volume fraction, an increase is obviously seen in the SiCp accumulation at the interface as a result of the increased particle size.

### 3.4. Fractography

Figure 7 illustrates the images of the fracture surfaces resulting from the tensile test for the friction-welded specimens S2 and S5. Examining the fracture surface images, fractures resulting from the tensile test were on the MMCs side, and it was observed that a brittle fracture mechanism was seen. For MMC, the fracture shape was an intergranular crack which was special to brittle fracture. At the low tensile strength, the fracture features are of cleavage, while for high tensile strength the features of fracture contain ductile micro-gaps. Similar trends were noted in the tensile specimens.

### 3.5. EDS analysis

SEM micrographs and EDS analysis of the friction welded joint S3 are presented in Fig. 8 and EDS analysis results of specimen S3 is also given in Table 3. Point 1 (on MMC side), point 2 (deformed zone), point 3 (fully plasticity deformed zone), point 4 (deformed zone) and point 5 (on AA 6061 side) are marked as the EDS analysis region. The elemental analysis and microstructural examination in the interface region of friction welded joint of S3 clearly indicated that different amounts of Al, Cu, C, O, Na, Mg and Si elements were obtained. From the results of EDS analysis taken from specimen S3, it was observed that the elemental

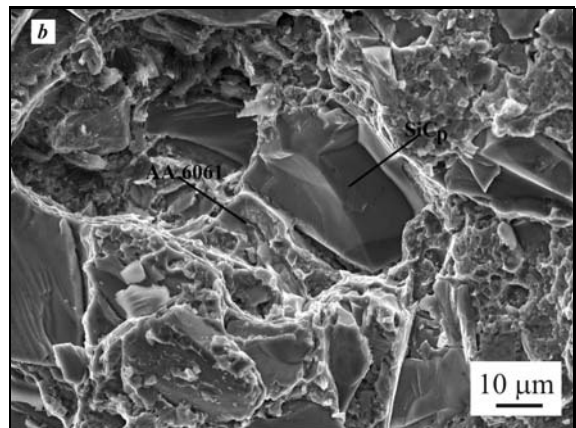
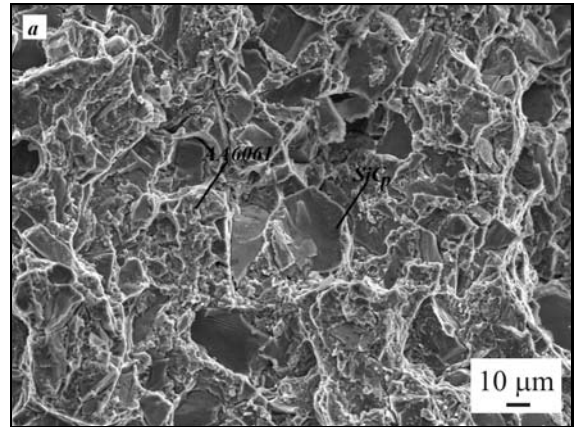


Fig. 7. SEM micrographs of fracture surfaces after tensile test of friction-welded S2 (a) and S5 (b) specimens.

aluminum transition occurred from AA 6061 alloy to MMC. Furthermore, carbon transition occurred in the same distance from MMC to AA 6061 aluminum alloy.

## 4. Conclusions

The study determined the effect of particle size and volume fraction on the weldability of metal matrix composites (MMCs) to AA 6061 aluminum alloy by using friction welding. Based on this work, the following conclusions can be drawn:

1. In this study, SiCp particle reinforced Al-based MMCs were successfully joined to AA 6061 aluminum alloy by friction welding. Microstructural analyses showed substantially defect-free joints. This paper presents the report on successful application of friction welding to join MMCs. In particular, the experimental results demonstrated FW to be an attractive welding technology for particle reinforced Al-based MMCs.

2. Microstructural studies of metal matrix composite/aluminum alloy friction welded joints revealed three different regions of the weld interface, i.e., unaffected zone (UZ), deformed zone (DZ), as well as a transformed and recrystallized fully deformed zone

Table 3. Quantity of concentration taken from EDS analyses across the welding interface of S3 specimen

EDS point	Alloying elements (wt.%)						
	Mg	Na	Si	C	O	Cu	Al
1	2.90	0.64	14.71	11.92	10.27	4.54	60.09
2	1.14	0.64	13.84	10.34	10.24	3.49	60.49
3	1.40	2.24	6.37	10.64	10.13	2.37	67.84
4	1.37	2.24	3.36	10.24	9.62	1.26	71.32
5	1.32	2.38	0.31	8.49	7.99	1.02	89.0

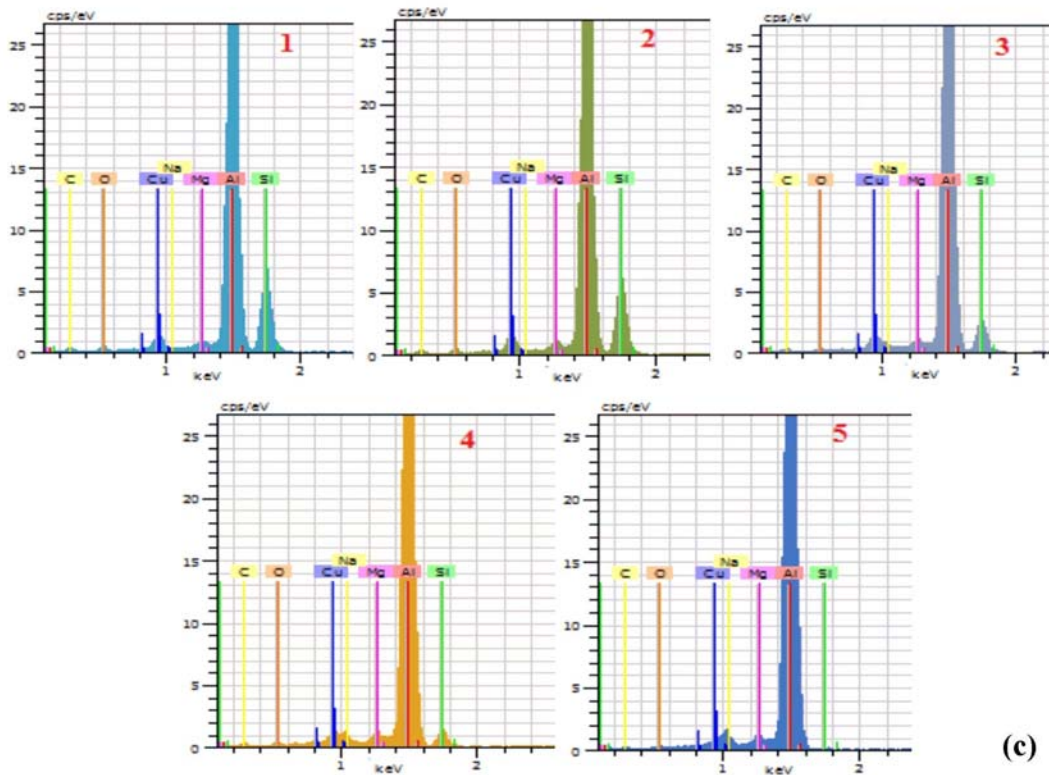
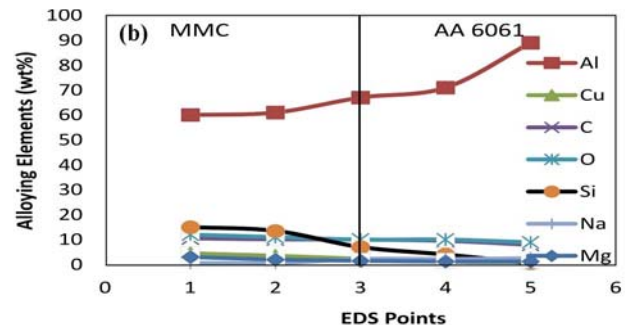
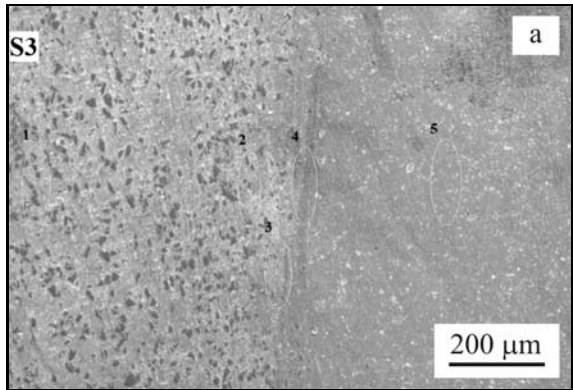


Fig. 8. SEM micrographs (a) and EDS analysis (b, c) of the friction welded joint S3.

(FPDZ). However, these areas were characteristically different with increasing particle size and volume fraction of SiCp.

3. From the results of the tensile test, the highest tensile strength of FW joints was carried out as  $345 \text{ N mm}^{-2}$  for S1 specimen. Compared the FW

joints with each other, there is an important difference: the tensile strength depends on the increase of reinforced SiCp particle size and volume fraction. Additionally, all the FW joints presented the same fracture behavior since all the failures in the tensile specimens were located in the MMCs side. The results of fractography of S2 and S5 sample indicated that a brittle fracture mechanism and an intergranular crack on the MMCs side were observed.

4. The EDS analysis of S3 sample indicated that different amounts of Al, Cu, C, O, Na, Mg and Si elements were obtained. It was observed that the elemental Al transition occurred from AA 6061 to MMC, while C transition occurred in the same distance from MMC to AA 6061 aluminum alloy.

### References

- [1] Di Ilio, A., Poletti, A.: *Int J Mach Tool Manuf*, 40, 2000, p. 173.
- [2] Han, N. L., Yang, J. M., Wang, Z. G.: *Scripta Mater*, 43, 2000, p. 801. [doi:10.1016/S1359-6462\(00\)00492-9](https://doi.org/10.1016/S1359-6462(00)00492-9)
- [3] Zhang, X. P., Ye, L., Mai, Y. W., Quan, G. F., Wei, W.: *Composites Part A*, 30, 1999, p. 1415. [doi:10.1016/S1359-835X\(99\)00040-8](https://doi.org/10.1016/S1359-835X(99)00040-8)
- [4] Wang, M. Z., Xu, Z. C., Du, X. C., Pan, L. X.: *Met Sci Technol*, 10, 1991, p. 98.
- [5] Sammaiah, P., Tagore, G. R. N.: *Journal of Advanced Manufacturing Technology*, 3, 2009, p. 21.
- [6] Chattopadhyay, R.: *Advanced Thermally Assisted Surface Engineering Process*. Massachusetts, Kluwer Academic Publishers 2004.
- [7] Ozdemir, N.: *Materials Letters*, 55, 2005, p. 2504. [doi:10.1016/j.matlet.2005.03.034](https://doi.org/10.1016/j.matlet.2005.03.034)
- [8] Gerlich, A., Su, P., North, T. H., Bendzack, G. J.: *Materials Forum*, 29, 2005, p. 290.
- [9] Uday, M. B., Ahmad Fauzi, M. N., Zuhailawati, H., Ismail, A. B.: *Material Science and Engineering A*, 528, 2011, p. 1348. [doi:10.1016/j.msea.2010.10.060](https://doi.org/10.1016/j.msea.2010.10.060)
- [10] Jayabharath, K. et al: *Materials Science and Engineering A*, 454–455, 2007, p. 114. [doi:10.1016/j.msea.2006.11.026](https://doi.org/10.1016/j.msea.2006.11.026)
- [11] Hascalik, A., Orhan, N.: *Materials & Design*, 28, 2007, p. 313.